corrosion and materials degradation

MDPI

Article

Microbial Communities Associated with Alternative Fuels in Model Seawater-Compensated Fuel Ballast Tanks

Lina E. Dominici [1,*], Kathleen E. Duncan [2,*], Mark A. Nanny [3], Irene A. Davidova [2], Brian H. Harriman [2] and Joseph M. Suflita [2]

[1] Centro de Investigación y Desarrollo en Tecnología de Pinturas (CIDEPINT), CICPBA-CONICET-UNLP, La Plata B1900AYB, Argentina
[2] Department of Microbiology & Plant Biology, University of Oklahoma, Norman, OK 73019, USA
[3] School of Civil Engineering and Environmental Science, University of Oklahoma, Norman, OK 73019, USA
* Correspondence: l.dominici@cidepint.ing.unlp.edu.ar (L.E.D.); kathleen.e.duncan-1@ou.edu (K.E.D.)

Abstract: The biocorrosion of carbon steel poses a risk for ships combining seawater and fuel in metal ballast tanks. Ballast tanks were simulated by duplicate reactors containing carbon steel coupons and either petroleum F76 (petro-F76), Fischer–Tropsch F76 (FT-F76), or a 1:1 mix of both fuels, to investigate whether the alternative fuel FT-F76 influenced this risk. The polycarbonate reactors were inoculated with seawater, and the control reactors did not receive fuel. The reactors were monitored for 400 days, and they all reached a pH and open circuit potential where elemental iron was oxidized, indicating corrosion. The reactors containing petro-76 or fuel mix had higher levels of dissolved iron; one of each replicate had lower concentrations of sulfate than the original seawater, while the sulfate concentration did not decrease in the other incubations. The high sulfate reactors, but not the low sulfate reactors, had a high relative abundance of microaerophilic sulfide-oxidizing bacteria. The FT-F76 and the no-fuel reactors had a high relative abundance of iron-sequestering *Magnetovibrio*. Although dissolved iron and loss of sulfate under anoxic conditions are associated with biocorrosion, our results suggest that in our reactors these indicators were altered by iron-sequestering and sulfide-oxidizing microbes, which is consistent with the slow diffusion of oxygen across the polycarbonate reactors.

Keywords: biocorrosion; microbiologically influenced corrosion; petroleum F76 fuel; Fischer–Tropsch F76 fuel; ballast tank; fuel biodegradation; sulfide-oxidizing bacteria; magnetotactic bacteria

Citation: Dominici, L.E.; Duncan, K.E.; Nanny, M.A.; Davidova, I.A.; Harriman, B.H.; Suflita, J.M. Microbial Communities Associated with Alternative Fuels in Model Seawater-Compensated Fuel Ballast Tanks. *Corros. Mater. Degrad.* **2023**, *4*, 382–397. https://doi.org/10.3390/cmd4030020

Academic Editor: Daniel John Blackwood

Received: 28 April 2023
Revised: 26 June 2023
Accepted: 28 June 2023
Published: 3 July 2023

1. Introduction

Biocorrosion, or microbially influenced corrosion (MIC), often plays a preeminent role in many types of metal infrastructure damage [1–4]. While a variety of materials are subject to MIC, the biocorrosion of carbon steel is arguably of foremost concern. We investigated the biocorrosion of naval vessels that contain carbon steel ballast tanks that intentionally mingle fuel and seawater [5]. The fuel most commonly used by U.S. naval vessels is F76, also known as "military diesel" or petro-F76; it is a petroleum distillate. The U.S. Department of Defense recently undertook efforts to develop alternatives to the petroleum-based fuels, including plant-based and syngas [6,7] fuels. Alternative fuels must, like standard fuels, meet a variety of performance criteria [8,9], including biodegradability and corrosivity characteristics. It has long been known that the biocorrosion of fuel ballast tanks and other metal surfaces is of major concern, and the damage in some cases has been linked to the activity of sulfate-reducing bacteria [10,11].

The organizing principle of our investigation is that biocorrosion is influenced by: (i) the nature and activity of the microbial populations; (ii) the tendency for fuel to facilitate biodegradation; and (iii) the characteristics of the metal surfaces exposed to the microbes and fuel. Previous laboratory studies [9] compared the biodegradability of F76 fuels derived from plant-based materials and fuel derived from syngas by means of the Fischer–Tropsch process (FT-F76) with that of the traditional petro-F76. The plant-based F76 fuel

was the most easily biodegraded and the FT-F76 was the most resistant to decay under the experimental regimen. Liang et al. [9] proposed that the high relative abundance of branched alkanes (isoalkanes) in FT-F76 negatively influenced fuel biodegradability. The extent of biocorrosion was positively correlated with the loss of sulfate, implicating sulfate-reducing bacteria (SRB) as major contributors to MIC.

An earlier study on fuel-compensated naval ballast tanks with different fluid residence times and exposure to a single fuel (petro-F76) suggested that the microbial community succession and corrosion patterns reflected differences in the fuel biodegradation processes [5]. The microbial communities shifted from the diverse San Diego Bay seawater community profiles to less diverse compositions, with the early proliferation of Gammaproteobacteria. This was accompanied by an increase in the abundance of aerobic hydrocarbon-degradation genes and the detection of aerobic hydrocarbon metabolites. In contrast, when the fluids were held for up to 8 months, the ballast tank communities were dominated by Deltaproteobacteria (primarily SRB), and anaerobic hydrocarbon-degradation genes and the associated metabolites were readily detected. However, the rate of corrosion and the successional processes involved could only be inferred from the fluid residence time in individual ballast tanks and not from repeated samplings over time.

From a pragmatic standpoint, corrosion is easiest to detect when it occurs rapidly, but detection can be difficult when the rates are exceedingly slow, particularly in ballast systems where fluids can be retained for many months. Fundamentally, ballast tank corrosion involves the loss of iron from its elemental form to other forms that can be both soluble and insoluble. If a thermodynamic equilibrium is assumed, periodic monitoring of the chemical parameters (pH, open circuit potential (OCP), and changes in sulfate and sulfide concentrations) that influence the iron status may provide insight into the fate of iron and, thus, corrosion. The current study focuses on the value of such parameters and on the microbial communities that developed in duplicate constructed ballast tank model reactors containing carbon steel coupons, seawater, and fuels used by naval vessels. An issue with biocorrosion studies utilizing smaller incubations is that one metal coupon is used per incubation. Variability in metal coupons causes stress and strain during processing and handling, while manganese sulfide strands, as well as crystalline defects, produce differences in localized MIC [12–14]. Addressing this variability requires multiple replicates of samples. Even so, this variability in the metal coupon introduces uncertainty into the analysis of different replicate coupons when attempting to characterize biocorrosion results under "identical" replicate conditions.

In this study, increasing the reactor size allowed 24 coupons per reactor; secondly, there was enough liquid volume to conduct multiple analyses on the same sample, thereby ensuring that the microbial community and the resulting chemistry were a result of the same metal conditions. It has been strongly recommended that several lines of evidence be used to determine whether or not MIC has occurred [15]. A companion paper will separately report on the results of adding marine sediments to the reactors and incubating for another year before collecting samples from the coupons, water phase, and sediments.

2. Materials and Methods

2.1. Reactor Design

Duplicate reactors containing 24 coupons (1018 carbon steel, mill finish, Metal Samples, Munford, AL, measuring 1.3 cm × 7.6 cm × 0.15 cm) were inoculated with approximately 2550 mL seawater from San Diego Bay Harbor (San Diego, CA, USA) and a total of 120 mL of either petro- or FT-F76 fuel or a 50:50 mix of both fuels; there were also duplicate control reactors unamended with fuel (Figure 1). The fluid level within the reactors was designed such that the coupons were below the water–fuel interface and never in direct contact with fuel. Each reactor consisted of a 15 cm long polycarbonate tube (15.24 cm diameter, 0.5 cm thick) sealed at each end with a polypropylene cap. Polycarbonate was selected because of its relatively low oxygen permeability at 25 °C (67.9 cm^3 mm/m^2 day atm) [16]; its excellent chemical resistance to jet fuels and gasoline [17]; and its thermal stability [18],

thereby allowing autoclaving without loss of structural durability. Each cap used a nitrile O-ring to maintain an air-tight seal with the polycarbonate tube. The caps were secured by bolting them together using four threaded rods (0.6 cm diameter) external to, and extending the length of, the reactor (Figure 1). At the center of each cap, a threaded port allowed connection with a threaded Teflon adaptor designed to hold a septum with a crimp-top butyl rubber seal. Coupons were mounted parallel to the cylindrical axis on a polypropylene frame using nylon bolts. The total reactor volume was 2.7 L. The reactors were situated horizontally upon two rollers held in a frame and were rotated at 0.33 rpm using a variable motor. Rotation about the central axis was used to prevent a static two-phase system where a portion of the metal surface is exposed to the hydrocarbon phase and another to the aqueous phase, as well to an interface region. With rotation, the metal coupons remained in the aqueous phase at all times, and the motion provided continual stirring, preventing the particles from settling and mimicking, to some extent, the motion of a ship.

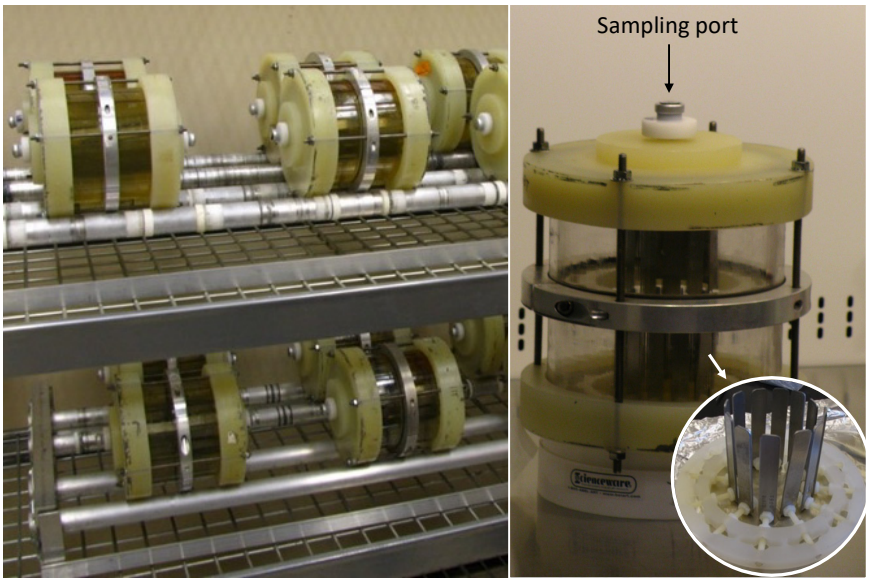

Figure 1. Ballast tank reactors on rotating platforms. Assembled reactor with 2 holders of coupons (24 coupons total). Reactors were filled with seawater from San Diego Bay. Holder with 1018 carbon steel coupons shown in the inset photo.

The coupons were cleaned, dried under a stream of N_2 gas, and autoclaved twice in Schott bottles as previously described [19]. The unassembled reactors, minus the coupons, were autoclaved then baked in an oven at 150 °C for 1 h. The autoclaved coupons were screwed into position in the reactors using sterile gloves and autoclaved tools, and the whole reactor was placed under UV light in a PCR hood for 15 min before the fill spout was attached. Air was pumped out via the sample port using a needle, flushed with sterile N_2 gas, and autoclaved once more. The reactors were dried overnight at 55 °C then placed in a laminar flow cabinet for inoculation. All the reactors were inoculated with untreated seawater obtained from San Diego Bay Harbor. Six reactors were amended with fuels that had been sterilized with a hydrophobic Teflon (0.22 mm) membrane filter (Millipore, [20]) and then made anoxic by prolonged flushing with N_2 gas (Table 1). The controls included two reactors without fuels. All the reactors were then filled with untreated seawater obtained from San Diego Bay Harbor.

The reactors were incubated on a rotating platform (1 rotation every 3 min) in the dark at a temperature between 18 and 22 °C. The reactors were allowed to become anoxic naturally via the activities of the aerobic and microaerophilic bacteria in the seawater that rapidly consume dissolved oxygen [21]. The reactors were visually inspected during each sample collection to ascertain whether the reactor fluid contained black precipitates, which would suggest the production of iron sulfides due to the activity of sulfate-reducing

microbes. All the samples were collected through a port closed with a butyl rubber stopper and secured by an aluminum crimp using a N_2-flushed sterile syringe. The volume of sample removed was replaced by filter-sterilized N_2 gas.

Table 1. Reactor composition and experimental design. Fuel and seawater were added at the start of the experiment. See Materials and Methods for further details.

Reactor #	Fuel Type
R1	Petro-F76
R2	Petro-F76
R3	FT-F76
R4	FT-F76
R5	Petro- and FT-F76
R6	Petro- and FT-F76
R7	No fuel
R8	No fuel

2.2. Chemical Analyses

Dissolved oxygen was measured immediately after sample collection using a Firesting-O_2 oxygen meter (Pyro Science GmbH; Aachen, Germany), operated according to the manufacturer's instructions. Dissolved sulfide was measured immediately after sample collection using the methylene blue method (Sulfide VACUettes kit K-9510D, CHEMetrics, Midland, VA, USA). The sulfate was quantified by ion chromatography as previously described [19]. For the determination of the dissolved metals, each sample was filtered with a 0.45 µm PES filter (Whatman Puradisc) and diluted to a metal concentration range between 0 and 40 mg per liter using 0.1% (*v/v*) nitric acid (Fluka, Ultrapure). The dissolved metal concentrations were measured as previously described [5].

Open circuit potential (OCP) and pH were measured in a 10 mL subsample transferred to a small crimp-sealed electrochemical cell using a syringe flushed with N_2 gas. All the OCP and pH measurements were made inside an anaerobic chamber with a 95% N_2 and 5% H_2 gaseous atmosphere. The open circuit potential was measured with an Ag/AgCl reference electrode and a platinum measurement electrode [22]. All the OCP data in the text, figures, and graphs are presented as values referenced to a standard hydrogen electrode (SHE). The pH measurements were obtained with an Orion 350 pH meter and Oakton pH electrodes. A three-point calibration curve, using pH buffer standards at pH = 4, 7, and 10, was used for each measurement.

2.3. Microbial Enumeration

Microbial cells were enumerated from unpreserved San Diego Bay seawater by direct epifluorescence microscopy under blue excitation using a micrometer grid on an Olympus BX-61 microscope. Fresh seawater was fixed using a 1/10 volume of 37% formaldehyde, and a dilution of the fixed samples was stained with 5 µL of 5 ng/mL 4,6-diamidino-2-phenylindole (DAPI) in the dark for 45 min at room temperature. The fixed cells were then filtered onto 0.22 µm, 25 mm diameter black-stained polycarbonate membrane filters (Sterlitech, Auburn, WA, USA). At least 30 fields were counted and averaged for each slide.

2.4. Sulfate Reduction Assay

The rates of sulfate reduction in the samples were measured using a previously described radiotracer technique [23]. In brief, the samples (10 mL, in triplicate) were taken from the experimental reactors with syringes flushed with N_2 and emptied into sterile anoxic bottles through butyl rubber stoppers. The samples were then supplemented with 2 µCi $Na_2{}^{35}SO_4$ per bottle from an anoxic sterile stock solution. The ^{35}S-sulfate amendments did not measurably change the original concentration of this anion in the samples. The

bottles were incubated for 7–8 days at room temperature (about 21 °C). Following the incubation period, the pool of total reduced inorganic sulfur compounds was extracted by chromium reduction, volatilized by strong acid, and trapped in 10% Zn-acetate solution. The amount of ^{35}S in an aliquot of the trap solution was quantified by scintillation counting.

2.5. Microbiological Sample Collection and DNA Extraction

One liter of seawater from San Diego Bay was filtered through a 0.1 um pore size PES filter (ThermoScientific, Carlsbad, CA, USA, Cat # 567-0010). Three liters was separately filtered to provide replicate samples of the inoculum seawater. The filters were placed in 50 mL sterile Falcon tubes with 2 mL DNAzol (DN127, Molecular Research Center, Inc., Cincinnati, OH, USA) and stored at −80 °C until DNA was extracted. Fluid samples (100 mL) from the reactors were collected on day 400. The reactor fluid samples were preserved for DNA extraction by first filtering through a 0.2 µm pore size PES filter (ThermoScientific, Carlsbad, CA, USA, Cat # 567-0020). The filters were then placed in 50 mL sterile Falcon tubes with 1 mL DNAzol (DN127, Molecular Research Center, Inc., Cincinnati, OH, USA) and stored at −80 °C until DNA was extracted.

For DNA extraction, the filters were placed inside a sterile Petri dish and shredded using autoclaved tweezers; added back to the 50 mL sterile centrifuge tubes with 1 mL nuclease-free water, 10 µL Proteinase K (>600 mAU/mL, Qiagen, Germantown, MD, USA), and 10 µL 10% sodium dodecyl sulfate (Sigma-Aldrich, St. Louis, MO, USA); vortexed briefly at maximum speed; and incubated at 50 °C for 30 min. The RNA lysis buffer and RNA dilution buffer (250 µL each) from the Maxwell®16 Tissue LEV Total RNA purification kit (Promega, Madison, WI, USA) and 1 tube of Lysing matrix beads E were added to the tube containing the filter and vortexed briefly at maximum speed, followed by subsequent bead beating for 2 min and centrifugation at 6000× *g* for 5 min. The supernatant was collected and loaded into two Maxwell cartridges to extract DNA using the Maxwell instrument programed to operate in DNA mode [24]. The two extractions were eluted in 100 µL nuclease-free water and pooled. The DNA was quantified by fluorometry using the Qubit® dsDNA HS Assay (ThermoScientific, Carlsbad, CA, USA). DNA extraction was repeated 2 more times in order to obtain a more representative sample of the microbial community, each time adding 500 µL nuclease-free water, 10 µL Proteinase K (>600 mAU/mL, Qiagen, Germantown, MD, USA), and 10 µL 10% sodium dodecyl sulfate (Sigma-Aldrich, St. Louis, MO, USA) to the original tube. The vortexing, incubation, addition of Maxwell buffers, etc., were performed as for the 1st extraction, but the supernatant was added to one Maxwell cartridge. All three DNA extractions were pooled, and the pool was used for qPCR and to construct 16S rRNA amplicon libraries.

2.6. Quantification of 16S rRNA Gene Copies by Quantitative PCR

The primers S-D-Arch-0519-a-S-15 and S-D-Bact-0785-b-A-18 [25] were used to estimate the total number of bacterial and archaeal 16S rRNA gene copies. The thermal cycling, data acquisition, and analyses were carried out with the StepOnePlus™ Real-Time PCR System and StepOne Software v2.1 (Life Technologies, Carlsbad, CA, USA). The qPCR reactions (15 µL) contained 7.5 µL of 2xSYBR®Green PCR Master Mix (Life Technologies, Carlsbad, CA, USA); 3 µL of RT-PCR H_2O; 0.75 µL of forward and 1.5 µL of reverse primers (at 100 micromole concentration); and 3 µL of either diluted DNA or RT-PCR H_2O (no template control). The cycling conditions began with a hot start (95 °C, 10 min), followed by 40 cycles (95 °C/30 s; 52 °C/45 s; 72 °C/45 s) with collection at 72 °C. A melt curve was generated at 95 °C/15 s; 60 °C/60 s, with collection (+0.3 s) at 95 °C/15 s). The efficiency% was 92.9%. For each qPCR run, a 1:10 dilution series of a control DNA plasmid containing a bacterial 16S rRNA gene sequence was used to generate a 7-point standard curve. The standards, no-template controls, and samples were assayed in triplicate.

2.7. Construction and Analysis of 16S rRNA Amplicon Libraries

An aliquot of DNA extracted from the samples was used to generate 16S amplicon libraries with distinctive barcodes as previously described [26]. Briefly, the M13-519F/785R primer set (specifically primers S-D-Arch-0519-a-S-15 and S-D-Bact-0785-b-A-18 [25]) was used to amplify the V3-V5 region of the 16S rRNA gene, and a 12 base pair sequence conjugated to M13 [27] was used to barcode each sample. The amplicon library was prepared for sequencing using the NEBNext® Ultra™ II DNA Library Prep Kit for Illumina® in the Oklahoma Medical Research Foundation Genomics Facility (Oklahoma City, OK, USA) and sequenced on the MiSeq platform using PE250 V2 chemistry. All the amplicon library sequences were deposited in the NCBI Sequence Read Archive under Bioproject accession number PRJNA875099.

The amplicon library sequences were processed using the open-source package DADA2 (Divisive Amplicon Denoising Algorithm) in R software version 4.2.1 [28,29]. Amplicon sequence variants (ASV) were inferred, and taxonomic affiliations were determined using the SILVA v132 database as the reference database. Microbial community analysis was performed on the rarefied samples to 3338 sequences using R packages. Alpha diversity indices were calculated based on the Hill number [30] using the HillR package. The number of reads before rarefaction and the alpha diversity measurements are summarized in Table S1. Beta diversity analysis was performed by principal coordinate analysis (PCoA) biplot based on the Unifrac weighted distance matrix using the phyloseq and ggplot2 packages [31,32] and by nested bar plot using the fantaxtic package [33] with phyloseq data.

2.8. Statistical Analysis

One-way ANOVA with Tukey's honestly significant difference and Dunnett (2-sided) post hoc tests were used to analyze the microbial community composition data at the genus level using Statistical Package for the Social Sciences (SPSS for Windows version 28.0.0, IBM, Chicago, IL, USA). The significance level was set at 0.05 for the post hoc tests, and the no-fuel reactors were designated as the control group in the Dunnett test.

3. Results

3.1. Chemical Analyses

3.1.1. OCP, pH, and Dissolved Oxygen

The dissolved O_2, pH, and OCP in the San Diego seawater used to inoculate the reactors were 7.00 ppm, 8.3, and 220 mV, respectively. The OCP and pH were monitored throughout the experiment to track the bulk redox conditions and changes in pH that might indicate microbial activity (Figure 2). Initially, all the reactors quickly lost oxygen and became more anoxic, as shown directly by the measured oxygen levels, and as inferred from the negative open circuit potentials. However, over time, the OCP for the "seawater only" and "FT-F76" reactors slowly increased. By day 400, (Figure 2), two groups were observed. Group 1 contained the Petro-F76 reactors (R1, R2) and the 50:50 mix reactors (R5, R6), with OCP values of −300 to −325 mV and pH values between 7.5 and 7.8. Group 2 contained the no-fuel reactors (R7, R8) and the FT-F76 reactors (R3, R4) with OCP values between −100 and −250 mV and pH values from 8.1 to 8.4. It was calculated that approximately 6×10^{-6} moles of oxygen diffused into a reactor per day [34], based on the oxygen permeability properties of the polycarbonate used in the construction of the reactor (see Materials and Methods for further details). If the rate of oxygen diffusing into the reactors was the same for all the reactors, then the maintenance of a lower OCP in the Group 1 reactors would suggest that the Group 1 reactors, which contained petro-F76 fuel, had a higher rate of oxygen consumption than the Group 2 reactors.

3.1.2. Sulfur Species

The sulfate concentration was 28.1 mM, and the H_2S concentration was 0 mM in the San Diego Bay seawater used for the inoculum. The changes in sulfate concentration were

monitored over the course of the experiment in the fluid phase by ion chromatography and the rates of sulfate reduction by radiometric tracer. As summarized in Figure 3a, all the reactors except R2 and R6 had lower concentrations of sulfate than the starting seawater by day 400.

The rates of sulfate reduction were significantly above the background levels for only one sample (R6: fuel mix, day 83, Table S2). Dissolved H_2S was never detected.

3.1.3. Dissolved Fe

The dissolved Fe concentration in the San Diego seawater was 16.2 ppb. Over the 400-day period, the dissolved Fe concentration in reactors 1, 2, 5, and 6 (Group 1—containing either petro-F76 or 50:50 mix) increased to values between 12,000 and 22,000 ppb (Figure 3b). Although reactors 3, 4, 7, and 8 (Group 2—containing either FT-F76 or no fuel) experienced an increase of up to 7000 ppb on day 83, by day 400 their dissolved Fe concentration was 1500 ppb or lower, indicating the precipitation of iron species (Figure 3b). A dark color was seen in the reactors soon after inoculation, which was consistent with iron precipitates being present. The reactor fluids became dark in R3, R4, R7, and R8 starting on day 18, while the remaining reactors became equally as dark by day 52. All the reactors contained black precipitates when the fluids were filtered at the end of the incubation.

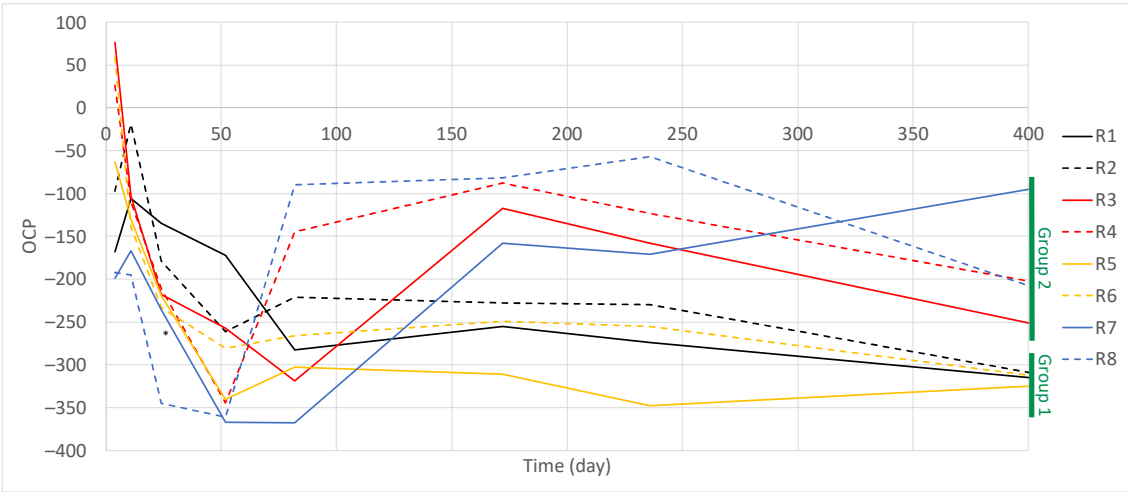

(**a**)

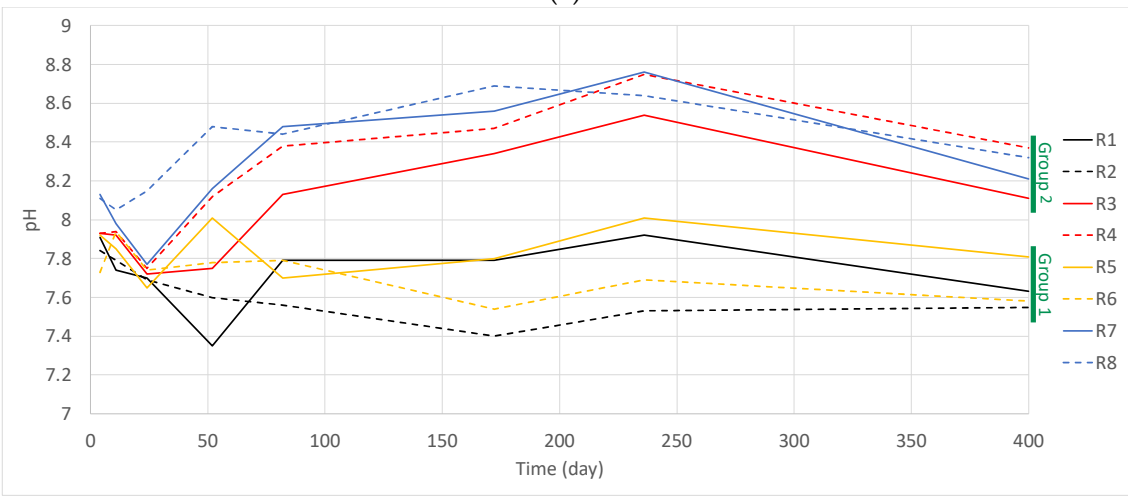

(**b**)

Figure 2. Parameter measurements. R1, R2: petro-F76 fuel; R3, R4: FT-F76 fuel; R5, R6: 1:1 mix of petro- and FT-F76 fuel; R7, R8: no fuel. (**a**) Open circuit potential (OCP, mV relative to SHE). (**b**) pH.

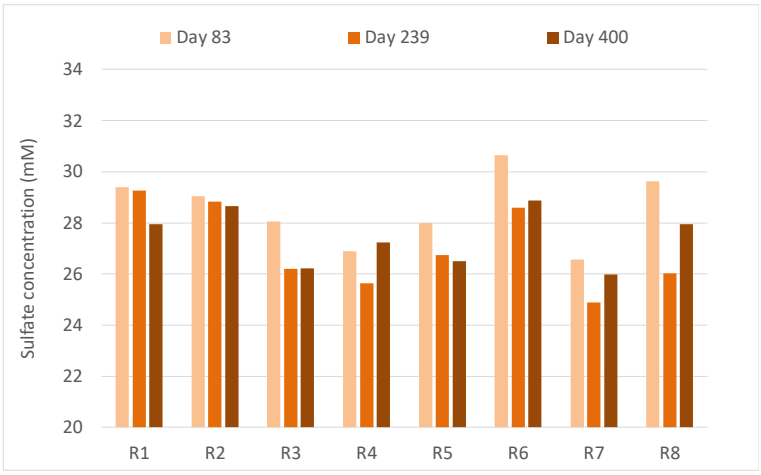

(**a**)

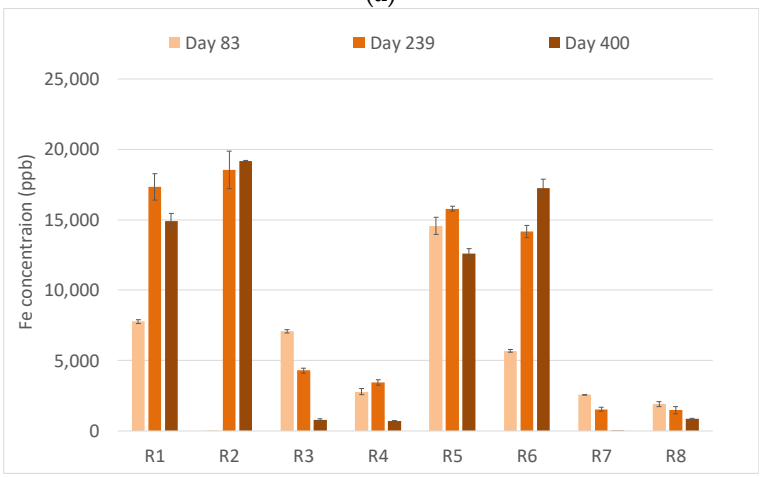

(**b**)

Figure 3. Dissolved chemicals. R1, R2: petro-F76 fuel; R3, R4: FT-F76 fuel; R5, R6: mix of petro- and FT-F76 fuel; R7, R8: no fuel added. (**a**) Sulfate concentrations (mM). (**b**) Iron concentration (ppb). Error bars indicate +/− 1 standard deviation.

3.2. Microbial Enumeration

3.2.1. Cell Counts

The concentration of cells in the San Diego Bay seawater used to inoculate the reactors was determined to be 1.95×10^6 (+/−0.32) cells/mL.

3.2.2. qPCR

The total number of bacteria and archaea in the water samples from the reactors was estimated after 400 days of incubation (Figure 4). The enumeration of bacterial and archaeal 16S rRNA genes in the seawater used to assemble the reactors was 1.05×10^6 gene copies mL^{-1}, which was similar to the cell counts mentioned above. The number of bacteria and archaea in the reactors was lower than that in the inoculum seawater and was estimated to range from 2.09×10^3 mL^{-1} (R1) to 2.6×10^5 mL^{-1} (R2). The replicate reactors that contained the same fuel amendments (R1:R2, R3:R4, R5:R6) differed greatly in the estimated number of 16S rRNA gene copies mL^{-1}.

3.3. Microbial Community Analysis: 16S rRNA Gene Amplicon Libraries

Microbial diversity indices, including species richness (q = 0 in the Hill number), exponential Shannon index (q = 1), and inverse Simpson index (q = 2, Table S1) of the communities in the reactors after 400 days of incubation showed lower species richness and diversity in the reactors than in the original seawater. The diversity index was higher

in the reactors with fuel than without fuel, with R1 and R2 (reactors containing petro-F76) being the most diverse and uniform, while the reactors containing any FT-F76 (e.g., R3, R4, R5, R6) were less diverse and uniform.

Figure 4. Quantification of copy number of 16S rRNA gene by qPCR in the inoculum seawater (SW1 and SW2) and the reactors (gene copies mL^{-1}). Error bars indicate +/−1 standard deviation.

3.3.1. Microbial Community Analysis of Reactor Water Samples

The microbial communities sampled from the water withdrawn from the reactors after 400 days of incubation differed from the inoculum seawater and each other. The dominant classes in the seawater (Figure 5) were Alphaproteobacteria (35%), Cyanobacteria (22.5%), Gammaproteobacteria (14%), and Bacteroidia (7.5%). The relative abundance of Cyanobacteria and Gammaproteobacteria (with the exception of R6) was much lower in the reactors than in the seawater. The reactors varied: R4, R7, and R8 had high relative abundance of Alphaproteobacteria (38–57%), while Campylobacteria were abundant in R2 and R6 (29%). Sulfate-reducing bacteria of the classes Desulfobacteria, Desulfovibrionia, and Desulfobulbia were higher in the reactors than in the seawater, with the highest relative abundance of these SRB in R3 and R5 (55–57%).

It was noteworthy that the microbial communities from the reactors containing fuel formed groups that did not reflect the type of fuel added (Figure 6). The no-fuel reactors (R7, R8) were similar in microbial community composition, including a high relative abundance of *Magnetovibrio*, and differed from the reactors containing fuel. The reactors containing fuel tended to have a lower relative abundance of Alphaproteobacteria and a higher relative abundance of Desulfobacteria and Desulfovibrionia (formerly classified as Deltaproteobacteria, Figure 5). However, the pairs of reactors that contained the same fuel did not have similar microbial communities and indeed were widely separated on the principal coordinates analysis (PCoA) graph (Figure 6). The reactors containing FT-F76 fuel, R3 and R4, differed particularly in that R4 had nearly 10 times the relative abundance of *Magnetovibrio* (22%) compared to R3, and R3 had 6 times the relative abundance of *Desulfobacter* (30%) compared to R4 (Figure 5). *Magnetovibrio* forms crystals of magnetite (Fe_3O_4), thus sequestering iron, and the cells contain sulfur inclusions when grown on sulfide or thiosulfate under microaerophilic conditions with oxygen as the terminal electron acceptor [35]. Each reactor with petro-F76 could be paired with a reactor containing a mix of fuel, with R1 being more similar to R5 and R2 to R6, suggesting that the influence of petro-F76 predominated over FT-F76, but at least two different communities formed in response to the petro-F76 fuel. The communities in reactors 2 and 6 were distinguished by Flavobacteriia, Alpha-, Gamma-, and especially Epsilonproteobacteria, which are capable of sulfur oxidation, and also by genera associated with hydrocarbon degradation. These genera include, *Lutibacter*, *Amphritea*, *Parvibaculum*, *Poseidonibacter*, *Marinobacter*, *Halarcobacter*, and members of the family Arcobacteraceae. The relative abundance of Syntrophotalea (formerly *Pelobacter*) was also highest in R2 and R6. *P. carbinolicus* [36] can use Fe(III) or S^0 as an electron acceptor.

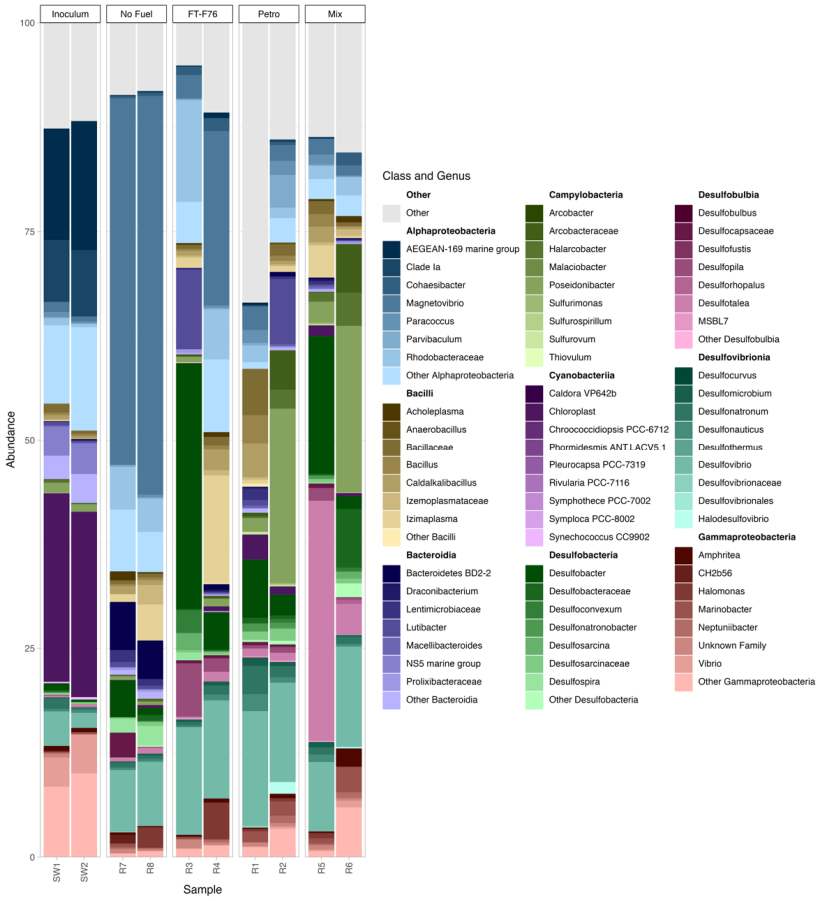

Figure 5. Bar plot using the top taxa to represent the relative abundance of the top 9 classes and the top 7 genera. Colors signify a top taxonomic rank (class) and a gradient of shades and tints signifies levels at a nested taxonomic rank (genus).

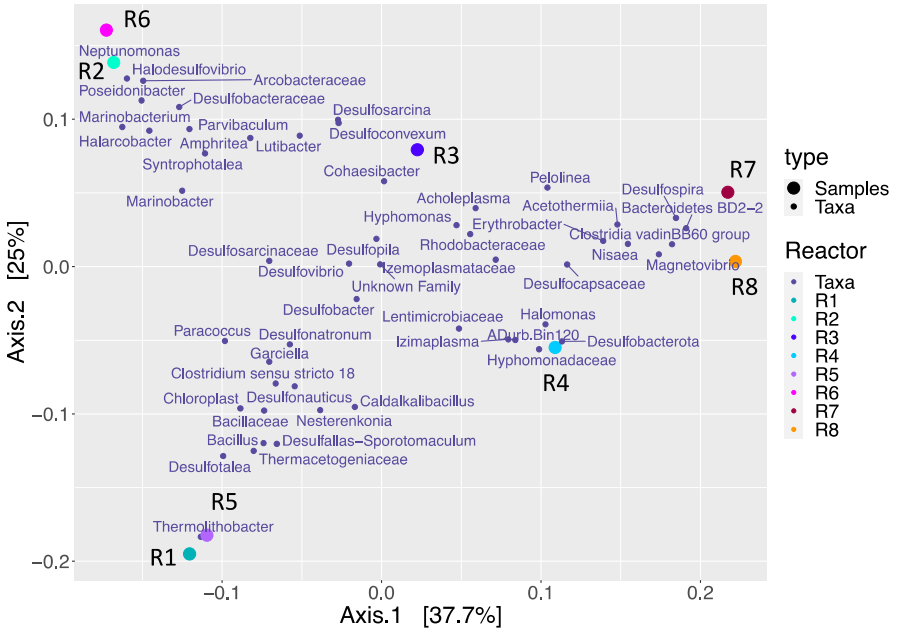

Figure 6. Principal coordinate analysis of the 16S amplicon libraries from water samples taken after 400 days of incubation at genus level with relative abundance > 1% using Unifrac weighted distances.

4. Discussion

This study used a laboratory model of fuel-compensated ballast tanks to assess the effects of specific fuels on the development of microbial communities that possibly biodegrade the fuels and impact microbially influenced corrosion.

4.1. Effect of Fuels on pH, OCP, Dissolved Iron Chemistry, and Sulfate Reduction

The type of fuel or its absence, in conjunction with the microbial community successional events, impacted the pH, OCP, and dissolved iron chemistry present in the reactors. The reactors containing petro-F76 (Group 1: R1, R2, R5, R6) maintained lower pH and OCP values than the reactors with FT-F76 or no fuel (Group 2: R3, R4, R7, R8). Although all reactors (except for R7) maintained pH and OCP values that were consistent with either Fe^{2+} or $Fe(OH)^{+}$, as the thermodynamically most favorable iron species, the Group 1 reactors had dissolved iron concentrations up to two orders of magnitude greater than that of the Group 2 reactors. The presence of dissolved iron indicates corrosion of carbon steel during the incubation process. Increased dissolved Fe concentrations (Figure 3b) were related to lower pH and OCP values (Figure 2, Group 1, R1, R2, R5, R6) suggesting that pH and OCP control the iron speciation between soluble Fe^{2+} and insoluble ferric oxides.

The maximum concentrations of dissolved iron displayed in Figure 3b (~20,000 ppb) represent about 2.3 mg of Fe loss per coupon in a reactor. Likewise, every 1 mM of sulfate lost represents 1.2 mg of Fe in FeS_2(s). Therefore, at maximum corrosion conditions, no more than 10–15 mg of iron per coupon was ever oxidized; thus, it is assumed that the general corrosion was very mild over the course of the experiment, although these values do not rule out the occurrence of pitting corrosion.

The presence of petro-F76 minimized the start of sulfate loss in the reactors. As previously shown in Figure 3a, all the reactors except R2 and R6 lost sulfate over time (e.g., 400 d), presumably by microbial reduction of this anion to sulfide, although the losses were small for R1 and R8. Dissolved H_2S was not detected in the reactors, although if any was generated it might have been bound by dissolved iron or other metals. Note that given the pH and OCP values of these reactors, the thermodynamically predominant iron species in the presence of sulfide was insoluble FeS_2(s). In addition, as discussed in Section 3.3.1, the reactors contained a variety of sulfide-oxidizing bacteria.

4.2. Effect of Fuels on Microbial Community Composition

The presence and type of fuel had a marked effect soon after inoculation, as discussed in Section 4.1. Some 400 days after inoculation, the reactors R1, R2, R5, and R6, all of which contained at least some petro-F76 fuel, were similar in their OCP and pH values (Figure 2), had relatively high levels of dissolved iron (Figure 3b), and were more acidic (pH 7.6–7.8, Figure 2) than the seawater used as the inoculum (pH 8.3). R1 and R5 differed from R2 and R6 in that the former two also had somewhat lower levels of sulfate than the original seawater, while the sulfate level in R2 and R6 remained close to or higher than that of the seawater (Figure 3a). The microbial community composition of these reactors differed, with R2 and R6 being similar in that they had a nearly 10-fold higher relative abundance (approximately 30%) of sulfide-oxidizing, microaerophilic Campylobacterota (formerly Epsilonproteobacteria) compared to R1 and R5 (Figure 5); their abundance was nearly equal to that of the Desulfobacterota. The prevalence of sulfide-oxidizing taxa, including those of Flavobacteriia and Alpha- and Gammaproteobacteria in the water samples from R2 and R6, was shown previously in Figure 6. Desulfobacterota (formerly Deltaproteobacteria) were relatively abundant in all four reactors, ranging from 28% relative abundance in R2, 34% in R1, and 40% in R6 to 63% in R5. Therefore, the genetic potential to carry out sulfate reduction was present, but R2 and R6 showed no net loss of sulfate after 400 days, perhaps due to the sulfides being reoxidized by the Campylobacterota and other sulfide oxidizers. In addition, iron-reducing bacteria may have affected the dissolved iron levels. *Syntrophotalea* (9.8% in R6, formerly *Pelobacter carbinolicus*) can use Fe(III) or S^0 as an electron acceptor [36]. R1 and R5 did not have the same sulfide oxidizers or taxa capable of Fe(III) reduction as

R2 and R6 had. R1 was distinguished by a relatively high abundance (9%, Figure 5) of members of the genus *Thermolithobacter*, chemolithotrophic Fe(III) reducers [37], while R5 had a high relative abundance (30%, Figure 5) of *Desulfotalea*, which can use sulfate or Fe(III) as electron acceptors [38].

The samples taken from reactors R3, R4, R7, and R8 were also grouped together with regard to OCP and pH values (Figure 2) and all had low levels of dissolved iron, as well as sulfate levels at or somewhat below that of the inoculum seawater. The OCP and pH levels were higher than those seen in the samples from R1, R5, R2, or R6, although the OCP values were negative. Although the relative abundance of Desulfobacterota was lower for R4, R7, and R8 than for R1, R5, R2, or R6, the estimated numbers of Desulfobacterota were higher in R3, R4, and R8 than in R1 and R5 due to the low 16S rRNA gene copy numbers in R1 and R5 (Figure 4). The estimated numbers of Desulfobacterota in R7 (1.4×10^3 mL^{-1}) were below those in R5 (9.44×10^3 mL^{-1}), but above those in R1 (6.7×10^2 mL^{-1}). In contrast, the estimated number (3.83×10^4 mL^{-1}) and relative abundance of Desulfobacterota in R3 was higher, at 58%. We acknowledge that the relative abundance or numbers of a particular microbe does not equate to its level of activity [4,39]. However, it is suggestive that R4, R7, and R8 also contained a high relative abundance (22–50%) of *Magnetovibrio* (Alphaproteobacteria: Rhodospirillaceae). *Magnetovibrio* forms crystals of magnetite (Fe_3O_4), which sequester iron, and the cells contain sulfur inclusions when grown on sulfide or thiosulfate under microaerophilic conditions with oxygen as the terminal electron acceptor [35]. Laboratory studies of bacteria which form magnetosomes, such as *Magnetovibrio*, have demonstrated that substantial amounts of iron could be taken up from the environment [35,40,41] and might partially explain the low levels of dissolved iron in these reactors. Zhang et al. [42] noted that *Magnetovibrio* increased in relative abundance in microcosms containing coastal seawater, sediment, and steel coupons which were unamended with crude oil, but did not increase in the microcosms amended with crude oil.

However, despite the substantial differences between the duplicate microbial communities described above, some genera were significantly more abundant in the reactors containing different fuels (Table S3: summary of one-way ANOVA with post hoc tests; Table S4: full table of descriptive statistics). In the reactors with no fuel (R7, R8), these taxa (Class: Genus or lower level taxon) were Bacteroidia: Bacteroidetes BD-2, Alphaproteobacteria: *Magnetovibrio*; with petro-F76 fuel (R1, R2), they were Campylobacteria: *Sulfurovum*, Chloroflexia: JG30-KF-CM45 (Family), Desulfobacteria: Desulfosarcinaceae, Desulfobulbia: MSBL7 (Family Desulfurivibrionaceae), Clostridia: *Dethiosulfatibacter*, Firmicutes: unclassified; and with FT-F76 (R3, R4), they were Alphaproteobacteria: *Hyphomonas*. Most differences in relative abundance were for the genera at less than 2% relative abundance, except for the high relative abundance of *Magnetovibrio* (avg. 47.8%) in the no-fuel reactors R7 and R8 (see Tables S3 and S4 for details and for other taxa). Though the significant genera listed above grouped more often with the FT-F76 than the petro-F76 reactors, it is noteworthy that the fuel mix reactors (R5, R6) had, nevertheless, average values that shifted somewhat towards the petro-F76 reactors, reflecting how the mixture of fuels also subtly affected the microbial community composition.

4.3. How Might Oxygen Affect Sulfate Reduction?

The low levels of sulfate reduction activity were unexpected given the relatively high relative abundance of SRB genera and conditions that were generally compatible with sulfate reduction (e.g., plentiful sulfate, moderate temperature, and salinity). However, as noted previously, there was a slow diffusion of oxygen through the polycarbonate housing of the reactors, which could have inhibited the activity of the SRBs through the oxygen sensitivity of certain metalloproteins and glycyl radical enzymes [43], while favoring oxygen-utilizing microbes. Both the dominant sulfide-oxidizing bacteria (Epsilonproteobacteria), which were present at high relative abundance in R2 and R6, and *Magnetovibrio*, which was also abundant in R7 and R8, and to a lesser extent in R4, are microaerophilic or can tolerate some oxygen [35,44,45]. The presence of these microaerophilic and aerobic

microbes, in some cases at high relative abundance, is consistent with an environment experiencing some oxygen. Sulfide-oxidizing bacteria could oxidize sulfide formed by the sulfate-reducing bacteria, recycling the sulfur to more oxidized sulfur species [44]. Indeed, Deng et al. [46], after injecting nitrate and nitrite into an oil field with high H_2S concentrations, noted that as H_2S concentration and SRB levels dropped, the relative abundance of both nitrate/nitrite reducers and sulfide-oxidizing bacteria rose. In our study, reactors 2 and 6 among the fuel-containing reactors were noteworthy for a high relative abundance of sulfide-oxidizing *Arcobacter* (Epsilonproteobacteria) and other taxa belonging to Alpha- and Gammaproteobacteria and Flavobacteriia with the potential for sulfide oxidation (Figures 5 and 6). Another explanation for sulfate reduction activity not being detected was that while the aqueous phase was sampled for such activity, a greater abundance of SRB could have been associated with biofilms and might have been the main site of sulfate reduction activity. As shown by an examination of bulk phase water and coupon surfaces with microsensors [47], redox values can vary tremendously over small spatial areas, and microbial communities definitely vary over small scales [48]. We are aware that microbial activity, including MIC, cannot be predicted by the relative abundance of various taxa [4,39], but we note that sampling only the liquid phase does omit potential alternative sites of sulfate reduction activity.

4.4. Divergence between Replicate Reactors

Although samples taken from the field are invaluable, by their nature they cannot aim for the degree of replication achieved in laboratory studies. Our paired reactors, which began with the same seawater and fuel, were similar in their OCP and pH measurements. However, they had diverged in microbial community composition by 400 days as well as in estimated numbers of 16S rRNA copy numbers, which likely influenced the differences seen between the pairs in terms of the loss of sulfate and the level of dissolved iron. Therefore, although the starting conditions were as similar as possible, there was not one invariant trajectory for the microbial community set by the inoculum, fuel, and metal; rather, stochastic factors appear to have played a role in the "track" followed. Changes in the microbial community would be expected to continue over time in response to changes in OCP, pH, and oxygen levels, any biodegradation of fuels, depletion of nutrients, etc. Note that the no-fuel paired reactors remained more similar to each other than the reactors containing fuel did to each other (Figures 2, 5 and 6). This higher degree of similarity suggests that the biodegradation of hydrocarbons may be a potent random factor promoting differences in microbial community profiles, perhaps due to low but not zero absolute numbers of hydrocarbon-degrading microbes in the seawater inoculum, especially anaerobic hydrocarbon degraders. We suggest acknowledging that stochastic factors add to the complexity of predicting MIC in a fuel/water/metal context.

5. Conclusions

Petro-F76-amended seawater reactors mimicking fuel-compensated ballast tanks developed different microbial community compositions, OCP, pH, and dissolved iron levels to those of the reactors amended with FT-F76 fuel or the control reactors that were not amended with fuel. However, two very different microbial communities developed in reactors containing petro-F76 fuel. A low rate of oxygen diffusion into the reactors permitted complex microbial communities to develop which, by oxidizing reduced sulfur compounds or sequestering iron, could confuse predictions of corrosion based on loss of sulfate or high levels of dissolved iron. These findings emphasize the need for direct assessment of corrosion on metal surfaces.

Supplementary Materials: The following supporting information can be downloaded at: https://www.mdpi.com/article/10.3390/cmd4030020/s1, Table S1: Alpha diversity measurements for 16S rRNA amplicon libraries, Table S2: Sulfate reduction activity, Table S3: Summary of ONE-WAY ANOVA post hoc tests of reactors according to fuel additions, Table S4: ONE-WAY ANOVA fuel effects, description and results.

Author Contributions: Conceptualization, M.A.N., J.M.S., I.A.D. and K.E.D.; methodology, M.A.N.; formal analysis, M.A.N., L.E.D., K.E.D., I.A.D. and B.H.H.; data curation, L.E.D., I.A.D., K.E.D. and B.H.H.; writing—original draft preparation, K.E.D. and L.E.D.; writing—review and editing, L.E.D., K.E.D., I.A.D., M.A.N., J.M.S. and B.H.H.; supervision, M.A.N., J.M.S., K.E.D. and I.A.D.; project administration, J.M.S.; funding acquisition, J.M.S. All authors have read and agreed to the published version of the manuscript.

Funding: This research was funded by the Office of Naval Research Award Number N000141010946.

Data Availability Statement: All amplicon library sequences were deposited in the NCBI Sequence Read Archive under Bioproject accession number PRJNA875099.

Acknowledgments: We would like to acknowledge the technical assistance of Athenia Oldham, Charles Primeaux, and Ravi Garimella. Joseph Suflita and Chris Marks collected the seawater used in these experiments. Commander Heidi Boose, USN, facilitated access to these samples.

Conflicts of Interest: The authors declare no conflict of interest.

References

1. Youssef, N.; Elshahed, M.S.; McInerney, M.J. Microbial processes in oil fields: Culprits, problems, and opportunities. *Adv. Appl. Microbiol.* **2009**, *66*, 141. [CrossRef] [PubMed]
2. Chaves, I.A.; Melchers, R.E.; Peng, L.; Stewart, M.G. Probabilistic remaining life estimation for deteriorating steel marine infrastructure under global warming and nutrient pollution. *Ocean Eng.* **2016**, *126*, 129–137. [CrossRef]
3. Skovhus, T.L.; Lee, J.S.; Little, B.J. Predominant MIC mechanisms in the oil and gas industry. In *Microbiologically Influenced Corrosion in the Upstream Oil and Gas Industry*; Skovhus, T.L., Enning, D., Lee, J.S., Eds.; CRC Press: Boca Raton, FL, USA, 2017; pp. 75–86. [CrossRef]
4. Little, B.J.; Blackwood, D.J.; Hinks, J.; Lauroc, F.M.; Marsili, E.; Okamoto, A.; Rice, S.A.; Wade, S.A.; Flemming, H.-C. Microbially influenced corrosion—Any progress? *Corros. Sci.* **2020**, *170*, 108641. [CrossRef]
5. Marks, C.R.; Duncan, K.E.; Nanny, M.A.; Harriman, B.H.; Avci, R.; Oldham, A.L.; Suflita, J.M. An integrated metagenomic and metabolite profiling study of hydrocarbon biodegradation and corrosion in navy ships. *NPJ Mater. Degrad.* **2021**, *5*, 60. [CrossRef]
6. Bartis, J.T.; Van Bibber, L. *Alternative Fuels for Military Applications*; Rand National Defense Research Institute: Santa Monica, CA, USA, 2011.
7. Zinoviev, S.; Müller-Langer, F.; Das, P.; Bertero, N.; Fornasiero, P.; Kaltschmitt, M.; Centi, G.; Miertus, S. Next-generation biofuels: Survey of emerging technologies and sustainability issues. *ChemSusChem* **2010**, *3*, 1106–1133. [CrossRef] [PubMed]
8. Stamper, D.M.; Lee, G.L. *The Explicit and Implicit Qualities of Alternative Fuels: Issues to Consider for Their Use in Marine Diesel Engines*; Technical Report NSWCCD-61-TR–2008/15; Naval Surface Warfare Center: West Bethesda, MD, USA, 2008.
9. Liang, R.; Aktas, D.F.; Aydin, E.; Bonifay, V.; Sunner, J.; Suflita, J.M. Anaerobic Biodegradation of Alternative Fuels and Associated Biocorrosion of Carbon Steel in Marine Environments. *Environ. Sci. Technol.* **2016**, *50*, 4844–4853. [CrossRef]
10. Klemme, D.E.; Leonard, J.M. *Inhibitors for Marine Sulfate-Reducing Bacteria in Shipboard Fuel Storage Tanks*; Memorandum Report 2324; U.S. Naval Research Laboratory: Washington, DC, USA, 1971.
11. Klemme, D.E.; Neihof, R.A. *Control of Marine Sulfate-Reducing Bacteria in Water Displaced Shipboard Fuel Storage Tanks*; Memorandum Report 2069; U.S. Naval Research Laboratory: Washington, DC, USA, 1969.
12. Avci, R.; Davis, B.H.; Rieders, N.; Lucas, K.; Nandasiri, M.; Mogk, D. Role of Metallurgy in the Localized Corrosion of Carbon Steel. *J. Miner. Mater. Charact. Eng.* **2018**, *6*, 618–646. [CrossRef]
13. Rieders, N.; Nandasiri, M.; Mogk, D.; Avci, R. New Insights into Sulfide Inclusions in 1018 Carbon Steels. *Metals* **2021**, *11*, 428. [CrossRef]
14. Avci, R.; Suflita, J.M.; Jenneman, G.; Hampton, D. Impact of Metallurgical Properties on Pitting Corrosion in High-Pressure Seawater Injection Pipeline. In *Failure Analysis of Microbiologically Influenced Corrosion*; Eckert, R.B., Skovhus, T.L., Eds.; CRC Press: Boca Raton, FL, USA, 2021. [CrossRef]
15. Wade, S.A.; Webb, J.S.; Eckert, R.B.; Jenneman, G.E.; Rice, S.A.; Skovhus, T.L.; Sturman, P.; Kotu, S.P.; Richardson, M.; Goeres, D.M. The role of standards in biofilm research and industry innovation. *Int. Biodeterior. Biodegrad.* **2023**, *177*, 105532. [CrossRef]
16. Massey, L.K. *Permeability Properties of Plastics and Elastomers—A Guide to Packaging and Barrier Materials*, 2nd ed.; William Andrew Publishing/Plastics Design Library: Oxford, UK, 2003.
17. Cole-Parmer. Chemical Compatibility Database. Available online: https://www.coleparmer.com/chemical-resistance (accessed on 16 April 2023).
18. Kholodovych, V.; Welsh, W.J. Thermal-Oxidative Stability and Degradation of Polymers. In *Physical Properties of Polymers Handbook*, 2nd ed.; Marks, J.E., Ed.; Springer Science: New York, NY, USA, 2007; pp. 927–938.
19. Liang, R.; Suflita, J.M. Protocol for Evaluating the Biological Stability of Fuel Formulations and Their Relationship to Carbon Steel Biocorrosion. In *Hydrocarbon and Lipid Microbiology Protocols*; McGenity, T., Timmis, K., Nogales, B., Eds.; Springer: Berlin/Heidelberg, Germany, 2015; pp. 211–226. [CrossRef]

20. Suflita, J.M.; Aktas, D.F.; Oldham, A.L.; Perez-Ibarra, B.M.; Duncan, K. Molecular tools to track bacteria responsible for microbiologically influenced corrosion. *Biofouling* **2012**, *28*, 1003–1010. [CrossRef]
21. Lee, J.S.; Ray, R.I.; Little, B.J.; Duncan, K.E.; Aktas, D.F.; Oldham, A.L.; Davidova, I.A.; Suflita, J.M. Issues for storing plant-based alternative fuels in marine environments. *Bioelectrochemistry* **2014**, *97*, 145–153. [CrossRef] [PubMed]
22. Nordstrom, D.K.; Wilde, F.D. Reduction-oxidation potential (electrode method). In *Techniques of Water-Resources Investigations*; U.S. Geological Survey: Reston, VA, USA, 2005. [CrossRef]
23. Ulrich, G.A.; Krumholz, L.R.; Suflita, J.M. A rapid and simple method for estimating sulfate reduction activity and quantifying inorganic sulfides. *Appl. Environ. Microbiol.* **1997**, *63*, 1627–1630. [CrossRef] [PubMed]
24. Oldham, A.L.; Drilling, H.S.; Stamps, B.W.; Stevenson, B.S.; Duncan, K.E. Automated DNA extraction platforms offer solutions to challenges of assessing microbial biofouling in oil production facilities. *Appl. Microbiol. Biotechnol. Express* **2012**, *2*, 60. [CrossRef]
25. Klindworth, A.; Pruesse, E.; Schweer, T.; Peplies, J.; Quast, C.; Horn, M.; Glöckner, F.O. Evaluation of general 16S ribosomal RNA gene PCR primers for classical and next-generation sequencing-based diversity studies. *Nucleic Acids Res.* **2013**, *41*, e1. [CrossRef]
26. Oldham, A.L.; Sandifer, V.; Duncan, K.E. Effects of sample preservation on marine microbial diversity analysis. *J. Microbiol. Methods* **2019**, *158*, 6–13. [CrossRef] [PubMed]
27. Hamady, M.; Walker, J.; Harris, J.; Gold, N.J.; Knight, R. Error-correcting barcoded primers for pyrosequencing hundreds of samples in multiplex. *Nat. Methods* **2008**, *5*, 235–237. [CrossRef] [PubMed]
28. Callahan, B.J.; McMurdie, P.J.; Rosen, M.J.; Han, A.W.; Johnson, A.J.A.; Holmes, S.P. DADA2: High-resolution sample inference from Illumina amplicon data. *Nat. Methods* **2016**, *13*, 581–583. [CrossRef] [PubMed]
29. R Core Team. *R: A Language and Environment for Statistical Computing*; Version 4.2.1; R Foundation for Statistical Computing: Vienna, Austria, 2022; Available online: https://www.R-project.org/ (accessed on 23 June 2022)
30. Hill, M.O. Diversity and Evenness: A Unifying Notation and Its Consequences. *Ecology* **1973**, *54*, 427–432. [CrossRef]
31. McMurdie, P.J.; Holmes, S. Phyloseq: An R package for reproducible interactive analysis and graphics of microbiome census data. *PLoS ONE* **2013**, *8*, e61217. [CrossRef]
32. Wickham, H. *ggplot2: Elegant Graphics for Data Analysis*, 2nd ed.; Springer: New York, NY, USA, 2016.
33. Teunisse, G.M. Fantaxtic-Nested Bar Plots for Phyloseq Data. 2022. Version 2.0.1. Available online: https://github.com/gmteunisse/Fantaxtic (accessed on 10 March 2023).
34. Stern, S.A.; Fried, J.R. Permeability of Polymers to Gases and Vapors. In *Physical Properties of Polymers Handbook*, 2nd ed.; Marks, J.E., Ed.; Springer Science: New York, NY, USA, 2007; pp. 1033–1050.
35. Bazylinski, D.A.; Williams, T.J.; Lefèvre, C.T.; Trubitsyn, D.; Fang, J.; Beveridge, T.J.; Moskowitz, B.M.; Ward, B.; Schübbe, S.; Dubbels, B.L.; et al. *Magnetovibrio blakemorei* gen. nov., sp. nov., a magnetotactic bacterium (Alphaproteobacteria: Rhodospirillaceae) isolated from a salt marsh. *Int. J. Syst. Evol. Microbiol.* **2013**, *63*, 1824–1833. [CrossRef]
36. Lovley, D.R.; Phillips, E.J.; Lonergan, D.J.; Widman, P.K. Fe(III) and S^0 reduction by *Pelobacter carbinolicus*. *Appl. Environ. Microbiol.* **1995**, *61*, 2132–2138. [CrossRef] [PubMed]
37. Sokolova, T.; Hanel, J.; Onyenwoke, R.U.; Reysenbach, A.L.; Banta, A.; Geyer, R.; González, J.M.; Whitman, W.B.; Wiegel, J. Novel chemolithotrophic, thermophilic, anaerobic bacteria *Thermolithobacter ferrireducens* gen. nov., sp. nov. and *Thermolithobacter carboxydivorans* sp. nov. *Extremophiles* **2007**, *11*, 145–157. [CrossRef] [PubMed]
38. Knoblauch, C.; Sahm, K.; Jørgensen, B.B. Psychrophilic sulfate-reducing bacteria isolated from permanently cold arctic marine sediments: Description of *Desulfofrigus oceanense* gen. nov., sp. nov., *Desulfofrigus fragile* sp. nov., *Desulfofaba gelida* gen. nov., sp. nov., *Desulfotalea psychrophila* gen. nov., sp. nov. and *Desulfotalea arctica* sp. nov. *Int. J. Syst. Bacteriol.* **1999**, *49*, 1631–1643. [CrossRef] [PubMed]
39. Beech, I.B.; Gaylarde, C.C. Recent Advances in the Study of biocorrosion-an overview. *Rev. Microbiol.* **1999**, *30*, 177–190. [CrossRef]
40. Bazylinski, D.A.; Lefèvre, C.T.; Schüler, D. Magnetotactic Bacteria. In *The Prokaryotes: Prokaryotic Physiology and Biochemistry*, 4th ed.; Rosenberg, E., DeLong, E.F., Lory, S., Stackebrandt, E., Thompson, F., Eds.; Springer: Berlin/Heidelberg, Germany, 2013; pp. 453–494. [CrossRef]
41. Amor, M.; Tharaud, M.; Gélabert, A.; Komeili, A. Single-cell determination of iron content in magnetotactic bacteria: Implications for the iron biogeochemical cycle. *Environ. Microbiol.* **2020**, *22*, 823–831. [CrossRef]
42. Zhang, Y.; Zhai, X.; Guan, F.; Dong, X.; Sun, J.; Zhang, R.; Duan, J.; Zhang, B.; Hou, B. Microbiologically influenced corrosion of steel in coastal surface seawater contaminated by crude oil. *NPJ Mater. Degrad.* **2022**, *6*, 35. [CrossRef]
43. Lu, Z.; Imlay, J.A. When anaerobes encounter oxygen: Mechanisms of oxygen toxicity, tolerance and defence. *Nat. Rev. Microbiol.* **2021**, *19*, 774–785. [CrossRef]
44. Muyzer, G.; Kuenen, G.; Robertson, L.A. Colorless Sulfur Bacteria. In *The Prokaryotes: Prokaryotic Physiology and Biochemistry*, 4th ed.; Rosenberg, E., DeLong, E.F., Lory, S., Stackebrandt, E., Thompson, F., Eds.; Springer: Berlin/Heidelberg, Germany, 2013; pp. 555–588. [CrossRef]
45. Pérez-Cataluña, A.; Salas-Massó, N.; Diéguez, A.L.; Balboa, S.; Lema, A.; Romalde, J.L.; Figueras, M.J. Revisiting the Taxonomy of the Genus Arcobacter: Getting Order from the Chaos. *Front. Microbiol.* **2018**, *9*, 2077. [CrossRef]
46. Deng, S.; Wang, B.; Su, S.; Sun, S.; She, Y.; Zhang, F. Dynamics of Microbial Community and Removal of Hydrogen Sulfide (H_2S) Using a Bio-Inhibitor and Its Application under the Oil Reservoir Condition. *Energy Fuels* **2022**, *36*, 14128–14135. [CrossRef]

47. Schwermer, C.U.; Lavik, G.; Abed, R.M.; Dunsmore, B.; Ferdelman, T.G.; Stoodley, P.; Gieseke, A.; de Beer, D. Impact of nitrate on the structure and function of bacterial biofilm communities in pipelines used for injection of seawater into oil fields. *Appl. Environ. Microbiol.* **2008**, *74*, 2841–2851. [CrossRef]
48. Marks, C.R.; Cooper, J.T.; Bonifay, V.; Stamps, B.W.; Le, H.M.; Harriman, B.H.; De Capite, A.; Brown, K.R.; Aktas, D.F.; Sunner, J.; et al. Integrated Methodology to Characterize Microbial Populations and Functions Across Small Spatial Scales in an Oil Production Facility. In *Microbiologically Influenced Corrosion in the Upstream Oil and Gas Industry*; Skovhus, T.L., Enning, D., Lee, J.S., Eds.; CRC Press: Boca Raton, FL, USA, 2017; pp. 325–350. [CrossRef]